

Metronomic Photodynamic Therapy as a New Paradigm for Photodynamic Therapy: Rationale and Preclinical Evaluation of Technical Feasibility for Treating Malignant Brain Tumors[¶]

Stuart K. Bisland^{*1}, Lothar Lilge^{1,2}, Annie Lin¹, Robert Rusnov¹ and Brian C. Wilson^{1,2}

¹Ontario Cancer Institute, University Health Network, 610 University Avenue, Toronto, Canada M5G 2M9

²Department of Medical Biophysics, University of Toronto, 610 University Avenue, Toronto, Canada M5G 2M9

Received 5 March 2004; accepted 10 May 2004

ABSTRACT

The concept of metronomic photodynamic therapy (*mPDT*) is presented, in which both the photosensitizer and light are delivered continuously at low rates for extended periods of time to increase selective tumor cell kill through apoptosis. The focus of the present preclinical study is on *mPDT* treatment of malignant brain tumors, in which selectivity tumor cell killing *versus* damage to normal brain is critical. Previous studies have shown that low-dose PDT using 5-aminolevulinic acid (ALA)-induced protoporphyrin IX (PpIX) can induce apoptosis in tumor cells without causing necrosis in either tumor or normal brain tissue or apoptosis in the latter. On the basis of the levels of apoptosis achieved and model calculations of brain tumor growth rates, metronomic delivery or multiple PDT treatments, such as hyperfractionation, are likely required to produce enough tumor cell kill to be an effective therapy. *In vitro* studies confirm that ALA-*mPDT* induces a higher incidence of apoptotic (terminal deoxynucleotidyl transferase-mediated 2'-deoxyuridine 5'-triphosphate, sodium salt nick-end labeling positive) cells as compared with an acute, high-dose regimen (ALA-*aPDT*). *In vivo*, *mPDT* poses two substantial technical challenges: extended delivery of ALA and implantation of devices for extended light delivery while allowing unencumbered movement. In rat models, ALA administration via the drinking water has been accomplished at very high doses (up to 10 times therapeutic dose) for up to 10 days, and *ex vivo* spectrofluorimetry of tumor (9L gliosarcoma) and normal brain demonstrates a 3–4 fold increase in the tumor-to-brain ratio of PpIX concentration, without evidence of toxicity. After *mPDT*

treatment, histological staining reveals extensive apoptosis within the tumor periphery and surrounding microinvading colonies that is not evident in normal brain or tumor before treatment. Prototype light sources and delivery devices were found to be practical, either using a laser diode or light-emitting diode (LED) coupled to an implanted optical fiber in the rat model or a directly implanted LED using a rabbit model. The combined delivery of both drug and light during an extended period, without compromising survival of the animals, is demonstrated. Preliminary evidence of selective apoptosis of tumor under these conditions is presented.

INTRODUCTION

Phase-II clinical trials by us (1) and by Kaye *et al.* (2) have suggested enhanced survival when intracavitary photodynamic therapy (PDT) with hematoporphyrin derivative (Photofrin®; Axcan Pharma Inc., Mont Saint-Hilaire, Quebec, Canada) is used immediately after radical surgical resection of malignant brain tumors, such as glioblastoma multiforme (GBM). Randomized Phase-III trials to confirm this prospectively are in progress (3). However, clinical evidence of damage to normal brain tissue has also been observed (1). In a series of preclinical studies using tumors grown orthotopically in rabbit or rat brain, it was found that Photofrin-PDT is capable of destroying bulk intracranial tumor by hemorrhagic necrosis (4). However, despite a very low volume uptake of drug, normal brain tissues are exquisitely sensitive to Photofrin-PDT (5,6), probably, because of vascular endothelium damage in the intact blood-brain barrier (BBB). This is also true for several other photosensitizers, including tin ethyl etiopurpurin and aluminum phthalocyanine tetrasulfonate, meta-tetra(hydroxyphenyl)chlorin (mTHPC), the exception being protoporphyrin IX (PpIX) synthesized endogenously upon administration of 5-aminolevulinic acid (ALA) (ALA-PpIX), where the threshold for necrosis (7) in white matter is at least an order of magnitude higher than that for other drugs (8). Hence, ALA-PDT may be selective in destroying tumor *versus* normal brain tissue by necrosis. Acute, high-dose PDT (*aPDT*) also induces apoptosis in both intracranial tumor and normal brain tissue when mediated by Photofrin or ALA, and this is a stochastic rather than a threshold effect (8). Low-dose Photofrin-PDT, below the necrosis threshold, can also produce apoptosis in both tumor and normal brain tissue (9). However, current studies show that subthreshold, low-dose ALA-PDT can induce selective apoptosis of intracranial tumor cells, without

[¶]Posted on the website on 28 May 2004.

*To whom correspondence should be addressed: Ontario Cancer Institute, University Health Network, 610 University Avenue, Toronto, Ontario, Canada M5G 2M9. e-mail: sbisland@uhnres.utoronto.ca

Abbreviations: ALA, 5-aminolevulinic (hydrochloride) acid; *aPDT*, acute, high-dose PDT; BBB, blood-brain barrier; dUTP, 2'-deoxyuridine 5'-triphosphate, sodium salt; GBM, glioblastoma multiforme; LED, light-emitting diode; *mPDT*, metronomic PDT; MTD, maximum tolerated dose; mTHPC, meta-tetra(hydroxyphenyl)chlorine; i.p., intraperitoneal; PDT, photodynamic therapy; PI, propidium iodide; PpIX, protoporphyrin IX; TdT, terminal deoxynucleotidyl transferase; TUNEL, TdT-mediated dUTP nick-end labeling.

© 2004 American Society for Photobiology 0031-8655/04 \$5.00+0.00

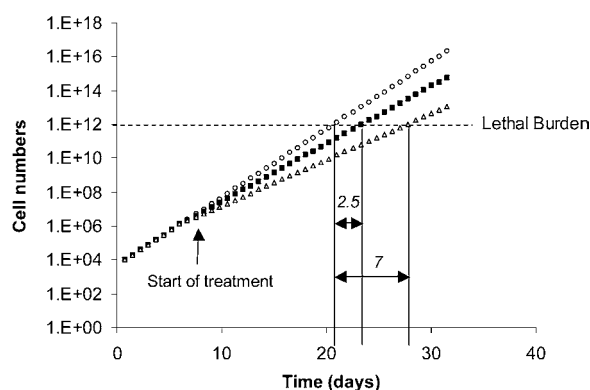


Figure 1. Hypothetical scheme of 9L cell burden with time: without treatment (○), with treatment providing 10% (■) and 20% (△) cell kill per cell doubling, giving a survival advantage of 2.5 and 7 days, respectively. Calculations are based on an 18 h cell doubling time starting with 5000 cells. Orthotopic 9L gliomas in rat typically cause death by 21 days after implantation if left untreated.

detectable damage (apoptotic or necrotic) to normal brain. This offers the possibility of treating patients with low-dose ALA-PDT after resection of bulk tumor as a means to achieve selective reduction of residual macroscopic tumor as well as microscopic nests of tumor cells that are responsible for the high recurrence rate after standard treatments.

On the basis of preliminary data, it seems unlikely that a single low-dose ALA-PDT treatment will provide an adequate level of selective tumor apoptosis to achieve tumor control. Hence, multiple treatments will be required. For example, with a cell doubling time of 18 h, the burden of a 9L gliosarcoma growing within rat brain typically becomes fatal by 21 days after implantation. Hypothetically, a treatment providing 10 or 20% cell kill per doubling could allow for a survival advantage of 2.5 and 7 days, respectively: see Fig. 1. Ultimately, the rate of cell doubling and the resulting total tumor volume burden determines the time to onset of clinical morbidity and mortality. It is, therefore, important to consider this when devising suitable dosing regimens aimed at achieving long-term tumor control.

Fractionated PDT is not a new concept. Repeat drug and light administration has been effective in, *e.g.* basal cell carcinoma (10). Alternatively, the light can be fractionated after a single photosensitizer dose, with the time intervals varied to achieve maximal photodynamic effect. Several studies using mTHPC or ALA have reported improved therapeutic results with light fractionation compared with single, acute treatments for both clinical and experimental cancers (11–13).

The term “metronomic” was recently introduced to describe continuous, low-dose administration of chemotherapeutic agents, after the discovery that low-dose chemotherapy is significantly more antiangiogenic than conventional high-dose regimens, with minimal side effects (14–16). There are many reports of toxicity and acquired resistance with conventional fractionated chemotherapy using maximum tolerated doses (MTD), leading to high morbidity and poor therapeutic response. Metronomic chemotherapy is under development as a method to minimize toxicity and prevent relapse. Metronomic PDT (*mPDT*) is proposed by analogy to this experience, although the underlying primary mechanisms are not the same because the principal rationale for *mPDT* is to improve the tumor-specific response. Nevertheless, acute, high-dose Photofrin-PDT has been shown to induce angiogenesis (17),

so that it will also be of interest in future studies to determine whether there is a comparable response after *mPDT*.

Here, we define *mPDT* as a treatment in which both the photosensitizer and light are administered during an extended period, either continuously at low rates or in many small, high-frequency fractions. Critical factors in this approach are that (1) the fraction of the remaining tumor killed in each time increment is sufficient to exceed the tumor regrowth rate and (2) especially for brain tumors, the tumor cell death is selective and primarily by apoptosis to avoid photodynamic damage (either apoptotic or necrotic) and secondary inflammation in response to necrosis. Hence, we hypothesize that *mPDT* could be safer and more selective than *aPDT*.

Previous reports have alluded to the possibility that a modified light or drug delivery (or both) regimen might prove beneficial. Jacques *et al.* (18) proposed administering ALA during an extended period to establish a higher equilibrium concentration of PpIX before irradiation. More recently, Madsen *et al.* (19,20) have shown a significant decrease in glioma cell survival *in vitro* after treatment with multiple drug–light fractions at intervals of 2 days as compared with the same total doses administered as an acute, single treatment. However, apart from our recent preliminary studies (21), to date there has been no report of extended-period, low drug and light dose rate PDT treatments targeted at selective apoptotic tumor kill.

mPDT presents two major technical challenges for clinical implementation: first, how to administer the photosensitizer continuously during an extended period (days–weeks, depending on the tumor doubling time) to ensure that a high equilibrium level of drug within the tumor is achieved while maintaining tumor to normal tissue selectivity and avoiding systemic toxicity? Second, how to deliver light continuously to the entire tumor in a minimally invasive way?

Previous evidence regarding the feasibility of extended ALA dosing is found in the work of Edwards *et al.* (22) who fed mice 10 $\mu\text{mol ALA kg body weight}^{-1}$ for 7 days via a subcutaneous peristaltic pump without causing loss of normal motor coordination, grip or nociception, which are signs of acute ALA-mediated porphyria (23). A similar study was conducted by Van de Boogert *et al.* (24) in rats given 200 mg kg^{-1} via bolus oral gavage without affecting normal liver or renal function. However, extended administration of ALA to patients can result in high ALA serum levels (23,25), so that drug toxicity is certainly a potential problem with *mPDT*. We have, therefore, initiated studies of extended ALA administration in rabbit and rat models to determine both the doses that can be tolerated without significant toxicity and the levels of PpIX achieved in brain tumor, normal brain and other tissues. Both multiple bolus injections and, for ease of administration, adding ALA to the drinking water have been tested.

Two different technical approaches are being developed for extended intracranial light delivery that involve the use of light-emitting diodes (LED) implanted directly into the brain cavity after tumor resection and either LED or low-power diode lasers that connect to interstitially placed optical fibers. The latter approach does not require prior surgical removal of the tumor. These delivery methods are being assessed in rabbit and rat models and the technical design and evidence of technical feasibility with irradiation during several days duration is presented. In both cases, the objective is continuous (or frequent intermittent) light delivery for days without compromising the ability of the animals to move about freely.

Finally, initial evidence is presented that, as with single low-dose PDT (26,27), ALA-induced PpIX-mediated *m*PDT can induce tumor-specific apoptosis without histological evidence of damage to normal brain.

MATERIALS AND METHODS

In vitro studies. *m*PDT and *a*PDT experiments were conducted using the murine-derived gliosarcoma 9L cell line. Cells (2 to 5×10^4) were plated into sterile 35 mm petri dishes (Nalge Nunc International, Rochester, NY) and incubated at 37°C , 5% CO_2 in the presence of complete growth media containing 10% fetal bovine serum (GIBCO, Grand Island, NY). Once adhered to the plates, cells were further incubated either in the presence or absence of 1 mM ALA for 4 h, at which time the light treatment commenced. A custom-designed light source was used, comprising six LED arrays (each of 25 LED; 635 ± 15 nm; Digi-Key Corp., Thief River Falls, MN) allowing simultaneous, continuous irradiation of six plates inside the incubator. Radiant exposure varied from 10 to $50 \text{ J cm}^{-2} \text{ day}^{-1}$ for up to 5 days duration using irradiances of $\leq 0.6 \text{ mW cm}^{-2}$. Irradiances were uniform to better than $\pm 5\%$ per well. Results presented are for *m*PDT with 10 J cm^{-2} at an irradiance of 0.116 mW cm^{-2} to provide continuous illumination during a 24 h period.

*a*PDT of comparable radiant exposure (10 J cm^{-2}) was delivered at a much higher irradiance of 21 mW cm^{-2} using a light source with a similar spectral emission. The irradiance of this light source could not be changed. At 6 h after *m*PDT or *a*PDT, cells were harvested from their dishes and prepared according to manufacturer's instructions for terminal deoxynucleotidyl transferase (TdT)-mediated 2'-deoxyuridine 5'-triphosphate, sodium salt (dUTP) nick-end labeling (TUNEL; Promega, Madison, WI) assay by flow cytometry as an indicator of apoptotic-specific DNA fragmentation of DNA. Propidium iodide (PI) staining was used to identify cells dying by necrosis. The functionality of the assay was confirmed using cisplatin treatment (18 h, $10 \mu\text{g mL}^{-1}$) as a positive control. Negative controls received light alone (10 J cm^{-2} during 1 day).

In vivo models. Two different tumor models were used, grown orthotopically by implanting tumor cells into normal brain. VX2 papilloma-derived squamous cell carcinoma in New Zealand White rabbits (5) has the advantage of providing a relatively large size brain, facilitating technology evaluation. VX2 was passaged intramuscularly in rabbits before being implanted as a cell suspension in the brain. The disadvantage is that it is not a glioma, although it does show several relevant morphological features of brain tumors such as microinvasion, growth along perivascular spaces and pseudopalisading. For rat models, 9L gliosarcoma were grown in immunocompetent, 6 week old male Fisher rats (170–200 g) (27). The 9L cells were maintained *in vitro* and harvested at 95% confluence during exponential growth phase.

After general anesthesia and craniotomy, cells were injected stereotactically below the intact dura to a depth of 2.5 mm (rat) or 5 mm (rabbit) using a 10 μL Hamilton syringe (cell numbers: VX2, 2×10^5 ; 9L, 5×10^3) in 5 μL saline. The craniotomies were covered with a sterile plastic sleeve, the scalp was sutured closed and the animals were allowed to recover. All surgeries were performed under aseptic conditions in a laminar flow hood. Analgesia (buprenorphine, 0.6–1 mg kg^{-1}) was administered as needed. Untreated tumors in the rabbit and rat typically grow to 5–8 mm and 2–3 mm diameter by Day 18 and 13, respectively. In the rabbit model, partial resection of the tumor was performed before the implantation of the LED light source. Resection was conducted under PpIX fluorescence image guidance, with excitation at 400 nm and collection between 600–650 nm, as described previously (28).

Metronomic drug delivery: toxicity and biodistribution in rat. ALA (1–10 mg mL^{-1} ; pH 6.5–3.7, hydrochloride; Frontier Scientific, Logan, UT) was administered either as an intraperitoneal (i.p.) bolus injections or via drinking water, in four different groups: either as a single injection or daily injections for 5 days, or in the drinking water for 1 or 5 days. Drinking water containing 1 mg mL^{-1} was equivalent to an ALA dose of $\sim 100 \text{ mg (kg day)}^{-1}$. Control animals did not receive ALA. All animals were maintained under minimal light conditions during their 12 h light cycle. The 1 and 5 days administrations commenced at 12 or 8 days after tumor implant, respectively. All animals receiving bolus injections were euthanized 4 h after the last injection, whereas those receiving ALA via the drinking water were euthanized at the allotted time points. An assessment of ALA toxicity was made by an observer blinded to the

experiment, scoring symptoms that included weight loss, lack of grooming, reddening of the eyes, disorientation, loss of balance and prolonged lethargy. Toxicity scoring was adapted from that devised by the Canadian Council on Animal Care (29). The MTD was taken as the ALA dose that did not lead to substantial weight loss ($<5\%$ difference from controls) after 5 days of drinking ALA (1 mg mL^{-1}).

The PpIX concentrations were measured in tumor, brain and several other tissues after administration of ALA at a dose of 100 mg kg^{-1} either as an i.p. injection or via the drinking water for 1 or 5 days. For this, the tissues were harvested immediately after sacrifice, snap frozen in liquid nitrogen and stored in the dark at -86°C until use. For assay, tissues were thawed, solubilized and the PpIX fluorescence measured by spectrofluorimetry, using a previously published technique that yields the PpIX concentration per gram tissue (30). This analysis was also performed blinded.

In vivo *m*PDT and light sources. PDT was commenced on Day 6 for the rabbit and Days 12 or 8 for the 1 or 5 days PDT treatment(s) in rat. For the rabbit model, an opening was made through the bone flap during the craniotomy into which an LED (635 ± 10 nm; Kingbright Corp., City of Industry, CA) was fixed using a bolt and screw attachment. The bone flap was then replaced and fixed with bone wax, and the skin sutured around the electrical lead. The LED sat within the partially resected tumor bed and was connected to the external power supply (Panasonic batteries, $2 \times 6 \text{ V}$), providing a total optical power of 6 mW. ALA 100 mg (kg day)^{-1} was administered intravenously via the marginal ear vein, followed 4 h later by light treatment consisting of 15 J day^{-1} fractions at intervals of 2 days for a total of 14 days.

In rats, light sources were designed to deliver the required irradiance at 635 nm to allow either *a*PDT or *m*PDT treatment for up to 5 days. On the basis of the toxicity study, rats were administered 100 mg kg^{-1} body weight ALA for 1 or 5 days, either as an i.p. bolus injection or via their drinking water. In all groups receiving PDT, animals were conditioned to ALA in their water for at least 4 days before the start of the light treatment to ensure adequate and consistent consumption followed by a 2 day ALA-free period between conditioning and the start of the ALA dosing for treatment. For *a*PDT light delivery, the initial target was to deliver 10 J interstitially to the tumor via an optical fiber, either as a single 50 min treatment at 3.3 mW in Group 1 or as five repeat treatments, each of 10 min duration for 5 days at 3.3 mW (2 J day^{-1}) in Group 2. For *m*PDT regimens, light was delivered continuously for 1 or 5 days at 115 μW (10 J day^{-1}) in Group 3, or 1 or 5 days at 23 μW (2 J day^{-1}) in Group 4. Subsequent *m*PDT treatments included higher fluence of 20 J (Group 5) and 50 J (Group 6) during periods of irradiation lasting from 1 to 5 days to increase the extent of apoptotic induction. For all irradiation protocols, the objective was to have the animal awake and moving freely throughout the irradiation period. The cage-mounted light source for fractionated delivery, seen in Fig. 2, comprises a diode laser or LED enclosed within a $9 \times 6 \text{ cm}$ plastic enclosure with a single external ON/OFF rocker switch connected to an optical fiber.

The laser diode is a 10 mW, 635 ± 5 nm (Sanyo DL4038-021; Thorlabs, Newton, NJ) with a prewired pin style-A driver kit (EK1101; Thorlabs). An external cooling fan is mounted above the diode enclosure (total weight 115 g). The driver (LD1100) can provide up to 250 mA in constant-power mode, providing $<0.01\%$ light-output stability. The fiber (multimode: 200 μm outer diameter, 0.39 numerical aperture) is directly coupled to the diode with silicon resin and the current is supplied either via a wall transformer (12 volts direct current, 300 mA; Digi-Key Corp.) or a 9 V alkaline battery. The diode–fiber coupling is secured onto the laser enclosure with a plastic collar, and the fiber is fed through a custom-designed swivel apparatus into a Kevlar-coated protective cladding (FT030: reinforced furcation tubing; Thorlabs). The Kevlar-coated fiber runs from the swivel to a backpack strapped to the back of the animal and recouples via a bare fiber terminal adaptor (ADASMA; Thorlabs) to a second short length of fiber implanted directly into the brain (tumor). Performance assessment using a spectrographic analyzer (00IBase32; Ocean Optics Inc., Winter Park, FL) showed that the cooling fan allowed continuous power output at 635 nm for $>1 \text{ h}$ with less than 2 nm shift in peak spectral emission.

For metronomic light delivery, a similar strategy to that described above was initially developed using LED (RED-Orange 5MM AlinGap 635 nm, 9000 mcd irradiance, 8° viewing angle; Kingbright) coupled to the 200 μm fiber via an ADASMA connector. The circuitry comprises a positive linear voltage regulator (UA78L09CLP; Digi-Key), together with two capacitors of 33 and 10 μF (35 V 1% RAD; part #s 399-1351/48-ND; Digi-Key Corp) and resistor (30 mA). Stable power output ($27 \mu\text{W} \pm <1\%$) for more than 24 h was achieved. The measured spectral range was $639.5 \pm 15 \text{ nm}$.

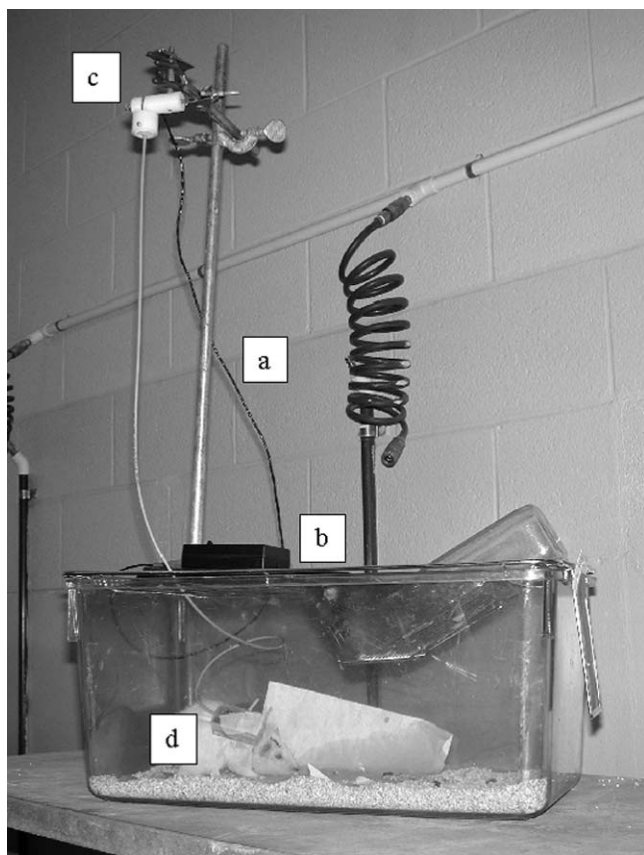
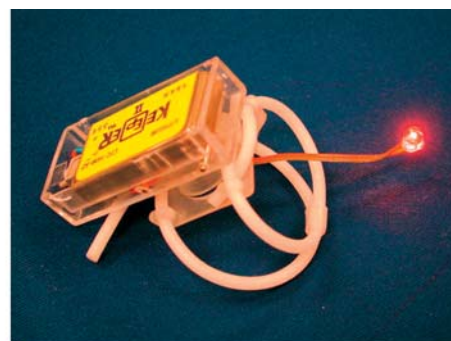


Figure 2. The cage-mounted, optical fiber-coupled diode laser for *mPDT* irradiation. The optical fiber (a) from the laser (b) runs through a swivel apparatus (c) into a backpack (d) on the rat for fiber-fiber coupling into the brain.

A significant improvement to the cage-mounted design was realized by constructing a battery-operated, tetherless “backpack” (Fig. 3A) weighing only 23 g that allows unrestricted movement throughout the *mPDT* treatment. The LED, fiber and circuitry is housed within a $5 \times 3.5 \times 2$ cm enclosure. The LED can be mounted into this housing via an SMA connector, allowing convenient reattachment of the fiber before and after each treatment. Alternatively, the LED can be secured onto the skull directly using bone cement to deliver the light transdurally (Fig. 3B). In either case, as with *aPDT*, the intracranial fiber is implanted and extends through a subcutaneous channel into the backpack. The backpack is powered by a lithium battery (Keeper Lithium LTC 16M-S2, 1700 mAh; Allied Electronics, Fort Worth, TX) with a single interchangeable resistor (33 or 100 ohms) and potentiometer (2 V) to regulate output. This gives a very stable power profile ranging from 1600 to 100 μ W for a 1–10 day continuous irradiation, respectively.

Histological analysis of PDT response. Animals were euthanized by intracardiac injection (Euthanyl; 0.5 mL, MTC Pharmaceuticals, Cambridge, Canada) 6 h after *aPDT* or immediately after *mPDT* treatment.

After sacrifice, the brain was removed intact, fixed in 10% formalin for 7 days, sectioned sagittally through the center of the PDT-treated region and embedded into paraffin. Multiple 4 μ m thick transverse sections were cut from each sagittal half and mounted onto slides. Sections were deparaffinized before staining for nuclear DNA fragmentation (apoptosis) using the TUNEL assay (DeadEnd Fluorometric TUNEL system; Promega) or the peroxidase *in situ* oligoligation assay (ApopTag ISOL, Serologicals Corp., Norcross, GA). For the former, positive control slides in each staining session were stained with 100 μ L DNase I® (Molecular Probes, Eugene, OR). Negative-staining controls were treated with fluorescein-12-dUTP® without TdT. Comparable controls were also used for the peroxidase staining. Fluorescent sections were subsequently immersed in 1 μ g mL⁻¹ PI (Molecular Probes) in phosphate-buffered solution containing calcium chloride and magnesium chloride to measure the total nuclear content. SlowFade™-Light Antifade



A



B

Figure 3. A: Tetherless *mPDT* backpack. The battery and potentiometer regulating the output of the light source are housed within the backpack. B: The electrical contacts and attaching LED are fed beneath the skin onto the skull. The animal is able to move freely around the cage throughout the *mPDT* procedure.

reagent (Molecular Probes) was added to prevent photobleaching before or during analysis. The samples were stored at 4°C in the dark until imaging.

Sections were imaged on a confocal laser-scanning microscope (CLSM 510, Carl Zeiss Canada Ltd, North York, Ontario, Canada), using sequential excitation and detection at 488 and 505–530 nm for fluorescein and 543 and >585 nm for PI.

RESULTS

mPDT-induced apoptosis *in vitro*

Figure 4 shows the flow cytometry results for 9L cells stained using TUNEL at 6 h after *aPDT* or *mPDT*. Of the gated cell populations (left column), the percentage of treated cells undergoing apoptosis, as discerned by the intensity of dUTP-fluorescein isothiocyanate labeling (middle column), was considerably greater after *mPDT* (51.3%; bottom row) than after *aPDT* (26.8%; lower middle row). In contrast, the percentage of necrotic cells (positive for PI; right column), was significantly greater after *aPDT* (36.8%) than after *mPDT* (2.7%). No effect on cell survival was seen after light treatment alone (top row) or drug alone (not shown). The ability for 9L cells to undergo apoptosis (99.1%) was confirmed after treatment with cisplatin (upper middle row).

Metronomic drug delivery *in vivo*

The consumption of drinking water containing ALA (1 mg mL⁻¹) was 25 ± 12 and 25 ± 14 mL day⁻¹ for 1 or 5 day regimens, respectively. This is equivalent to an ALA dose of 86 ± 2 and 137 ± 10 mg kg⁻¹ body weight day⁻¹, which did not appear to have

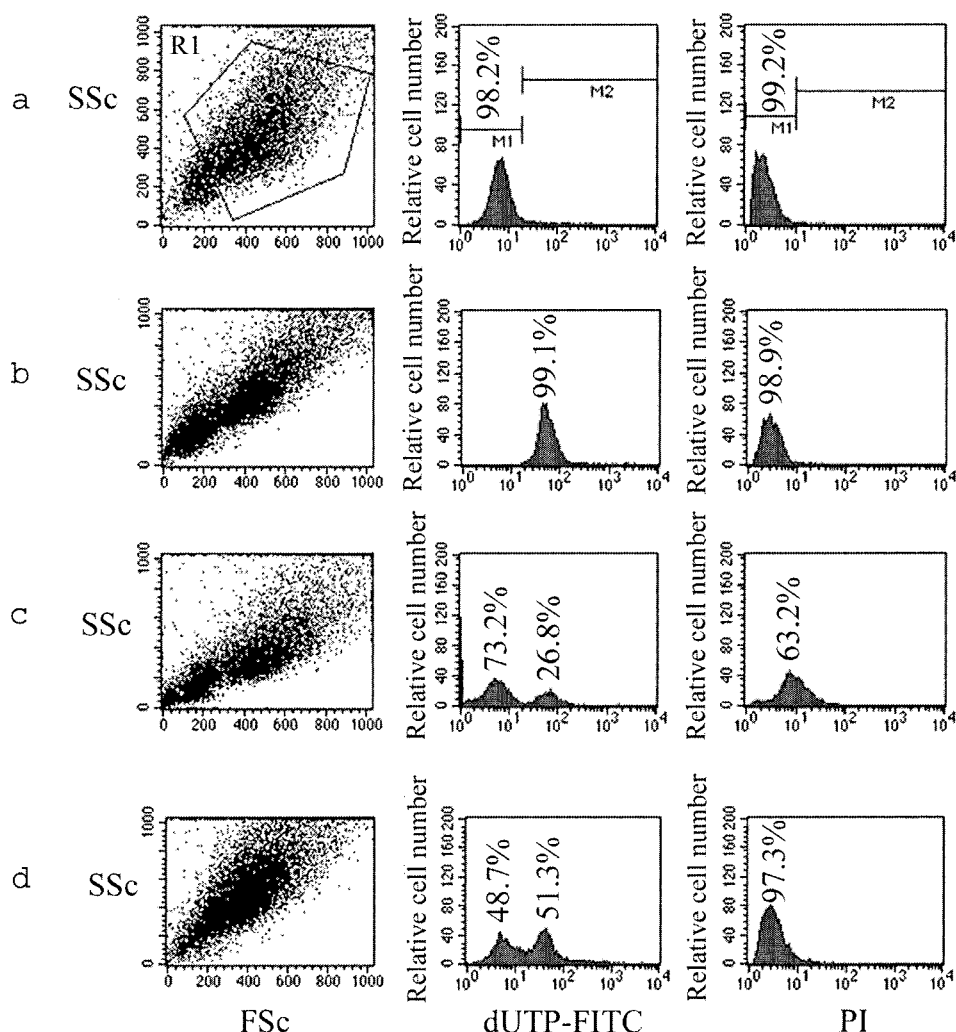


Figure 4. Flow cytometry analysis of PDT-induced apoptosis in 9L cells using TUNEL. Row a, negative control, light only (10 J cm^{-2} , 0.116 mW cm^{-2}); row b, positive control, cisplatin ($20 \mu\text{g mL}^{-1}$ for 18 h); row c, ALA- α PDT (10 J cm^{-2} @ 21 mW cm^{-2}); row d, ALA-mPDT (10 J cm^{-2} @ 0.116 mW cm^{-2}). dUTP-fluorescein isothiocyanate labeled (middle column): M1, nonapoptotic; M2, apoptotic. PI (right column): M1, alive; M2, dead (necrotic).

any significant effect on the health of the animals or on weight gain compared with controls. Figure 5 summarizes the toxicity assessment (27) of continuous drinking water administration of ALA in normal and 9L tumor-bearing rats. The latter were more prone to morbidity than non-tumor-bearing animals. The initial weight loss after tumor implant compounded the effects of ALA feeding, such that $>300 \text{ mg (kg day)}^{-1}$ ($\sim 2 \text{ mg mL}^{-1}$) led to notable weight loss within 5 days. A dose of $100\text{--}150 \text{ mg (kg day)}^{-1}$ ($\sim 1 \text{ mg mL}^{-1}$; pH 6.5) for 10 days did not result in toxicity outside the normal range in either tumor- or non-tumor-bearing animals. Moreover, nontumor animals did not show any signs of ill health for ALA doses up to $500 \text{ mg (kg day)}^{-1}$ for up to 10 days, although reduced weight gain after 5 days drinking was noted. However, $>600 \text{ mg (kg day)}^{-1}$ ALA resulted in continued weight loss during this same period. The highest ALA dose tested of $1000 \text{ mg (kg day)}^{-1}$ ($\sim 10 \text{ mg mL}^{-1}$; pH 3.7) was not tolerated by either tumor-bearing or non-tumor-bearing animals. Hence, the MTD during 10 days drinking was $\sim 500 \text{ mg (kg day)}^{-1}$ for normal rats and $\sim 150 \text{ mg (kg day)}^{-1}$ for tumor-bearing rats.

Biodistribution results of PpIX synthesis in ALA-treated ($100 \text{ mg [Kg day]}^{-1}$) animals are shown in Table 1. After 5 days, the

PpIX levels in tumor were approximately three- to four-fold higher than in normal brain tissue and significantly greater than for the other treatment groups. Encouragingly, given the potential for liver toxicity, the PpIX levels in liver for the 5 days continuous group were comparable with the controls. The liver concentrations were much higher when the ALA was given by bolus injection.

In vivo mPDT response

Figure 6 shows a representative TUNEL image of VX2 tumor-brain after mPDT using the implanted LED source. This reveals extensive tumor-associated apoptosis (bright spots, arrows). The incidence of apoptosis, although not solely confined to the tumor, is considerably less prevalent within normal brain. In the 9L rat model, a regimen of 1 mg mL^{-1} ALA (in the drinking water or i.p. bolus) followed by light at a dose rate of 2 J day^{-1} for 5 days (Groups 2 and 4) did not result in a noticeably higher level of apoptosis within the tumor beyond that found in control animals receiving either light treatment or ALA alone (results not shown). Similarly, the histological response for Groups 1 and 3 did not reveal pronounced PDT-induced apoptosis within tumor, although the incidence of

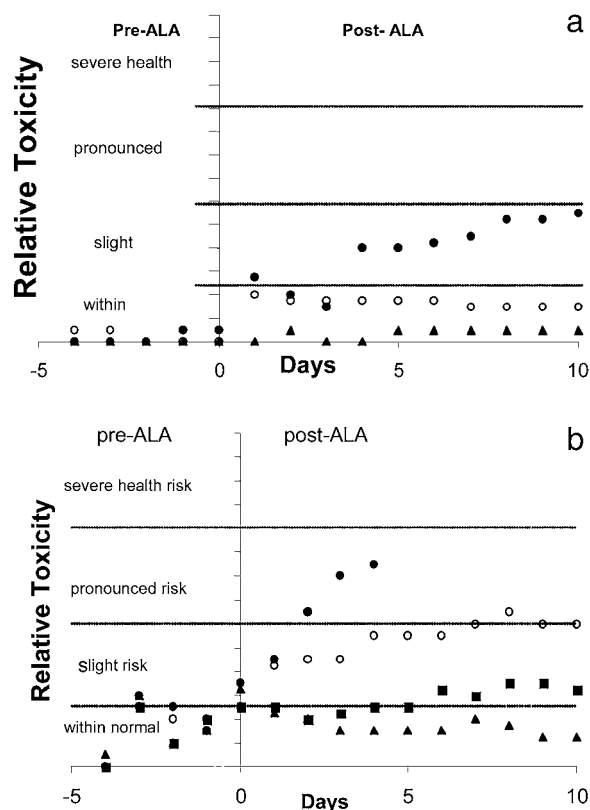


Figure 5. Toxicity as a function of number of days drinking ALA at three different dose levels (100–1000 mg/kg/day) for (A) non-tumor-bearing rats and (B) 9L tumor-bearing rats; concentration of ALA in the water 1(▲), 2 (■), 5(○) and 10 mg/mL (●).

apoptosis was increased for the same fluence delivered during 5 days compared with 1 day. However, apoptotic tumor cells were confined to the peripheral boundaries of the tumor, with few cells in either the outlying microfoci or the tumor centre.

By far the greatest *mPDT* response for 9L glioma in the rat was seen after a treatment of 50 J for 1 day. Figure 7A shows a low power magnification image of the tumor and surrounding normal cortex, revealing the preponderance of apoptosis within the tumor, most noticeably in microfoci (M; Fig. 7B) and around the periphery (Fig. 7C). Few apoptotic cells are evident within the normal cortex. It is also evident that the centre of the tumor is necrotic, and on the basis of qualitative evidence comparing similar tumor sections from animals that did not receive *PDT*, it is clear

Table 1. Tissue concentrations ($\mu\text{g g}^{-1} \pm 1 \text{ SD}$) of PpIX for different ALA administration regimens (bolus injection or drinking water) in 9L rats

	Liver	Brain	Tumor	Serum
Control	1.74 ± 1.00	0.42 ± 0.02	0.31 ± 0.01	0.055 ± 0.024
1× bolus injection	11.0 ± 1.2	0.70 ± 0.03	0.41 ± 0.02	0.074 ± 0.008
5× bolus injection	5.33 ± 3.26	0.24 ± 0.03	0.42 ± 0.03	0.14 ± 0.01
1 day drinking	0.34 ± 0.04	0.28 ± 0.01	0.39 ± 0.01	0.057 ± 0.008
5 day drinking	1.83 ± 1.25	0.56 ± 0.12	2.16 ± 0.55	0.066 ± 0.002

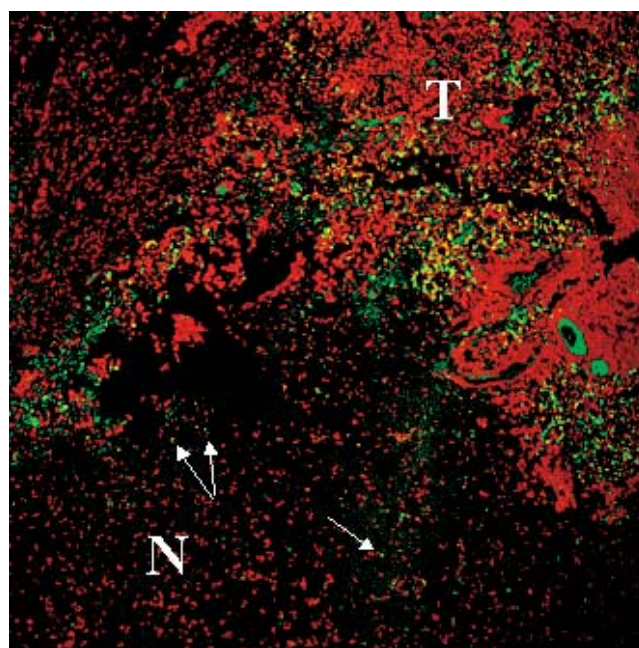


Figure 6. TUNEL-stained confocal micrograph of VX2 tumor (T) and adjacent normal brain (N) after fractionated ALA-*mPDT* (15 J day^{-1}) reveals extensive apoptotic bodies (bright spots) throughout the tumor with few in the normal tissue (arrows).

that the extent of necrosis is noticeably larger after *PDT*, suggesting that the necrosis is predominantly because of the *PDT* treatment and not as a result of poor vascular supply.

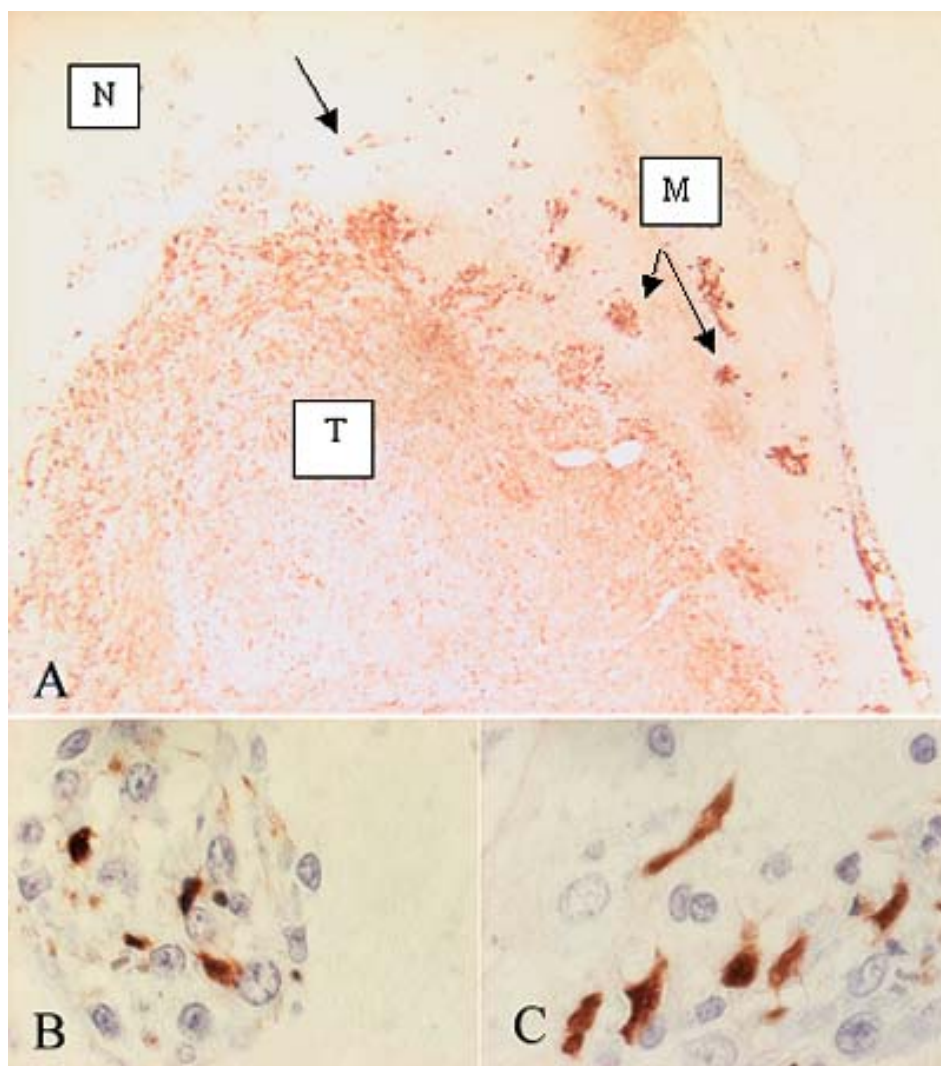
DISCUSSION

Our previous studies showed that high-dose ALA-*aPDT* (100 mg kg^{-1} intravenous [i.v.]; 50 J cm^{-2}) can induce necrosis in normal brain (cortex) as well as tumor (5), whereas an acute low-dose regimen (100 mg kg^{-1} i.v.; 5 J cm^{-2}) provides tumor-selective apoptosis without necrosis (8). This prompted us to hypothesize that perhaps *mPDT* with ALA could provide an even greater incidence of apoptosis of brain tumor cells without compromising selectivity.

We have shown here that ALA can safely be administered via the drinking water for at least 5–10 days continuously to normal, non-tumor-bearing rats and rats bearing 9L gliosarcoma at a dose ($\sim 100 \text{ mg [kg day]}^{-1}$) that is likely to be therapeutic, providing a high concentration of PpIX in tumor with high tumor to normal brain tissue selectivity (>3.8 -fold), higher than a comparable regimen of injections (1.7-fold). The absolute values of PpIX concentration in tumor ($2.16 \mu\text{g g}^{-1}$) are higher than those reported previously ($1.2 \mu\text{g g}^{-1}$ at 2 mg mL^{-1} ALA; 31), although as van den Boogert *et al.* aptly point out, there is considerable variability in reported ALA-induced PpIX levels in tumor, reflecting the differences in tumor models, implantation techniques and quantification assays (24). The use of prolonged ALA administration has been shown to be safe in patients with no evidence of resulting porphyrialike symptoms (23), supporting the potential application of ALA-*mPDT* clinically.

ALA represents the only known naturally occurring prodrug that can be administered orally to cause elevated synthesis of the endogenous photoactive compound PpIX as part of the heme

Figure 7. Horseradish peroxidase-labeled staining of apoptotic 9L tumor cells in the rat brain after ALA-*m*PDT (1 mg mL⁻¹; 50 J day⁻¹). A: Apoptosis is predominant at the tumor (T) periphery and microfoci (M) with conspicuous necrosis nearer the center. Few apoptotic cells are evident in the surrounding normal brain tissue (N), 100×. B: Out-lying microfoci containing apoptotic tumor cells, 400×. C: Apoptotic tumor cells at the periphery, 400×.



biosynthetic pathway (32). Moreover, the biodistribution of ALA (and hence PpIX) given orally is comparable with that after i.v. administration (24), and despite ALA being weakly acidic in solution, rats readily drink it in water at the required concentration without additional flavoring or buffering, after 1–2 days of conditioning. This is important because alkaline pH increases the propensity for ALA to degrade (22), so that buffering should be avoided when administering it via the drinking water. Equally vital is the ability of ALA to cross the BBB and thereby gain access to the tumor (33). ALA is a small, water-soluble molecule that can rapidly be absorbed across the BBB by mechanisms analogous to amino acid transport via pH-dependent ion pumps (34). Furthermore, the action of ALA-mediated PpIX is predominantly cellular, thus reducing the potential for PDT damage to the BBB (35).

The selectivity for ALA-mediated PpIX PDT is thought to reflect the heightened metabolism of rapidly dividing tumor cells as compared with the comparatively senescent neuronal cells of the normal brain. This results in a greater level of PpIX synthesis within tumor cells upon ALA administration. Therapeutic gain, in terms of survival or quality of life (or both), should be attainable with *m*PDT of the appropriate dosing provided that a sustainable level of tumor cell kill can be achieved that exceeds the rate of tumor cell doubling and consequently prevents or delays tumor

growth. The rapid cell doubling time of 9L cells (18 h) limits the survival time in the intracranial rat model (see Fig. 1), with little reprieve after a treatment that provides only 20% cell kill per cell doubling. However, a comparable cytotoxicity rate in patients could result in a better survival advantage because of considerably longer cell-doubling time (greater than five-fold).

This initial study describes a number of different light source strategies for facilitating *m*PDT *in vivo*, either low-power laser sources for *a*PDT treatments or LED-based sources for *m*PDT. Both strategies introduce technical challenges. A custom-made swivel apparatus was built to allow 360° rotation of the power cord and optical fiber without twisting or torque. However, even with Kevlar-coated tubing the rats were able to chew through the fiber and, despite the swivel mechanism, some degree of movement of the fiber at the entry point into the skull was inevitable, increasing the likelihood of mechanical damage. This was of particular concern during prolonged irradiation times. The animals tolerated well the cage-mounted laser source for the shorter treatment regimens, although the relatively poor fiber-to-fiber coupling efficiency limited the total power that could be delivered into the brain.

By far the best design for *m*PDT *in vivo* was the LED-based backpack. Above a weight of about 10% of body weight, the rats became agitated and then exhausted. With a lightweight, high-

energy battery, continuous stable output could be delivered for at least 10 days without complications and with high tolerance by the animals. The best results in terms of PDT response were obtained using the skull-mounted LED that provided transdural light delivery (Fig. 7), although the option for coupling the LED to an optical fiber also proved effective (results not shown). The skull-mounted LED has the advantage of reducing the likelihood of mechanical damage that may result from an interstitial fiber. For the rat model, direct implantation into the brain after resection is more challenging because of the small size but implanted LED microarrays may be feasible.

Using skull-mounted LED, acute or metronomic light treatments of 10 J day^{-1} in the 9L model were largely ineffective, whereas *mPDT* at 50 J day^{-1} resulted in substantial levels of apoptosis within the tumor and surrounding microfoci (Fig. 7). The VX2 rabbit model also showed considerable tumor-specific apoptosis after *mPDT*, which corroborates the efficacy of *mPDT* treatment using implantable LED. In both models, apoptosis was particularly conspicuous at the tumor periphery, an observation that has been reported previously by us using a similar glioma rat model after low-dose Photofrin-mediated *aPDT* (26). It is conceivable that these apoptotic cells represent the highly proliferative or leading edge of the tumor, where the oxygen supply is good and the tumor cell metabolism is not nutrient limited. Apoptosis is an adenosine triphosphate-dependent process and therefore is more likely in rapidly dividing cells where the vascular supply is not limiting. The total extent of apoptosis resulting from *mPDT* cannot be determined by histological assessment after treatment because the opsonized apoptotic cells are continually phagocytosed and removed from the lesion throughout the treatment. This results in an underestimation of the PDT response. Methods that allow real-time monitoring of apoptosis *in vivo* will undoubtedly prove useful in better quantifying the extent of apoptosis induced by *mPDT*. One such method allows the activation of apoptotic-specific enzymes to be monitored using bioluminescence (36), and we have recently shown that PDT responses in 9L tumor can be followed longitudinally in individual animals after PDT (37). However, similar to many tumors, including the VX2 carcinoma, gliomas are also susceptible to developing intrinsic necrosis and this will have to be differentiated from the effects caused by PDT.

Comparing metronomic and acute ALA-PDT *in vitro* reveals an almost two-fold enhanced incidence of apoptosis in 9L cells after *mPDT*. Interestingly, the levels of PpIX in the growth culture media after a single bolus administration of ALA (1 mM) remained elevated for up to 16 h, suggesting that PpIX synthesis saturates at this ALA concentration and exceeds the rate of PpIX photodegradation at the low radiant exposures used for *mPDT*. Further studies are planned to extrapolate more precisely the time course for apoptotic induction after either ALA-*aPDT* or ALA-*mPDT* as well as to determine the optimal metronomic dosing regimen for maximal apoptotic induction *in vitro*.

Currently, the options for treating malignant brain tumors are surgery followed by chemotherapy or ionizing radiation (or both). The primary goal of such regimens is to debulk the tumor mass, although they also aim to target distant microfoci that persist after surgical resection of the bulk tumor. Unfortunately, they are often ineffective at achieving the latter, resulting in high incidence of tumor recurrence. The results presented here confirm that *mPDT* can induce apoptosis in satellite microfoci without observable damage to normal brain and, in addition, maximizing the extent of apoptosis within these microfoci may be feasible, given the large

differential (>87-fold) in tumor *versus* white matter threshold for necrosis (5). This is of particular clinical relevance to GBM, which arises predominantly in white matter (38).

In summary, this study supports the concept and technical feasibility of developing ALA-*mPDT in vivo* as a treatment for brain tumors. Initial *in vitro* studies confirm the enhanced induction of apoptosis in 9L gliosarcoma cells after ALA-*mPDT* as compared with a similar *aPDT* regimen. Similar findings were made *in vivo*. Future work will address optimization of the drug and light delivery in similar glioma models that may more closely resemble gliomas in humans, notably U87 and CNS-1 tumors (39), as well as combining *aPDT* or *mPDT* (or both) with surgical resection using ALA-PpIX fluorescence image guidance resection (28). Other strategies include the combination of fluorescence-guided resection with *aPDT* or *mPDT* using other photosensitizers that have shown brain tumor responses and that are primarily apoptotic, such as 2-[1-hexyloxyethyl]-2-devinyl pyropheophorbide-a (40).

Acknowledgements—This work is supported by NIH grant PO1-CA43892 and by the Canadian Institutes of Health Research. Initial studies on low-dose ALA-PDT were supported by the Canadian Cancer Society through a grant from the National Cancer Institute of Canada. The authors acknowledge the important contributions of G. Netchev and E. Moriyama in the design and testing of the light sources.

REFERENCES

- Muller, P. J. and B. C. Wilson (1995) Photodynamic therapy for recurrent supratentorial gliomas. *Semin. Surg. Oncol.* **11**, 345–354.
- Kaye, A. H., G. Morstyn and D. Brownbill (1987) Adjuvant high-dose photoradiation therapy in the treatment of cerebral glioma: a phase 1–2 study. *J. Neurosurg.* **67**, 500–505.
- Muller, P. J., B. C. Wilson, L. Lilge, V. X. Yang, A. Varma, A. Bogaards, F. W. Hetzel, Q. Chen, T. Fullagar, R. Fenstermaker, R. Selker and J. Abrams (2002) Clinical studies of photodynamic therapy for malignant brain tumors: Karnofsky score and neurological score in patients with recurrent gliomas treated with Photofrin PDT. *Proc. SPIE* **4612**, 40–47.
- Chen, Q., B. C. Wilson, M. O. Dereski, M. S. Patterson, M. Chopp and F. W. Hetzel (1992) The effect of light fluence rate in photodynamic therapy of normal rat brain. *Radiat. Res.* **132**, 120–123.
- Lilge, L., M. C. Olivo, S. W. Schatz, J. A. MaGuire, M. S. Patterson and B. C. Wilson (1996) The sensitivity of normal brain and intracranially implanted VX2 tumor to interstitial photodynamic therapy. *Br. J. Cancer* **73**, 332–343.
- Lilge, L. and B. C. Wilson (1998) Photodynamic therapy of intracranial tissues: a preclinical comparative study of four different photosensitizers. *J. Clin. Laser Med. Surg.* **16**, 81–91.
- Patterson, M. S., B. C. Wilson and R. Graff (1990) *In vivo* tests of the concept of photodynamic threshold dose in normal rat liver photosensitized by aluminum chlorosulphonated phthalocyanine. *Photochem. Photobiol.* **51**, 343–349.
- Lilge, L., M. Portnoy, and B. C. Wilson (2000) Apoptosis induced *in vivo* by photodynamic therapy in normal brain and intracranial tumor tissue. *Br. J. Cancer* **83**, 1110–1117.
- Lilge, L., M. Sepers, J. Park, C. O'Carroll, P. Pournazari, J. Prosper and B. C. Wilson (1997) Preclinical studies of photodynamic therapy of intracranial tissues. *Proc. SPIE* **2972**, 64–73.
- Henderson, B. W., T. M. Busch, L. A. Vaughan, N. P. Frawley, D. Babich, T. A. Sosa, J. D. Zollo, A. S. Dee, M. T. Cooper, D. A. Bellier, W. R. Greco and A. R. Oseroff (2000) Photofrin photodynamic therapy can significantly deplete or preserve oxygenation in human basal cell carcinomas during treatment, depending on fluence rate. *Cancer Res.* **60**, 525–529.
- Muller, S., H. Walt, D. Dobler-Girdziunaite, D. Fiedler and U. Haller (1998) Enhanced photodynamic effects using fractionated laser light. *J. Photochem. Photobiol. B: Biol.* **42**, 67–70.
- Messmann, H., R. M. Szeimies, W. Baumler, R. Knuchel, H. Zirngibl, J. Scholmerich and A. Holsteg (1997) Enhanced effectiveness of

- photodynamic therapy with laser light fractionation in patients with esophageal cancer. *Endoscopy* **29**, 275–280.
13. van den Boogert, J., H. J. van Staveren, R. W. de Bruin, P. D. Siersema, and R. van Hillegersberg (2001) Fractionated illumination for oesophageal ALA-PDT: effect on blood flow and PpIX formation. *Lasers Med. Sci.* **16**, 16–25.
 14. Hanahan, D., G. Bergers and E. Bergsland (2000) Less is more, regularly: metronomic dosing of cytotoxic drugs can target tumor angiogenesis in mice. *J. Clin. Investig.* **105**, 1045–1047.
 15. Kerbel, R. S., G. Klement, K. I. Pritchard, and B. Kamen (2002) Continuous low-dose anti-angiogenic/metronomic chemotherapy: from the research laboratory into the oncology clinic. *Ann. Oncol.* **13**, 12–15.
 16. Browder, T., C. E. Butterfield, B. M. Kraling, B. Shi, B. Marshall, M. S. O'Reilly and J. Folkman (2000) Antiangiogenic scheduling of chemotherapy improves efficacy against experimental drug-resistant cancer. *Cancer Res.* **60**, 1878–1886.
 17. Ferrario, A., K. F. von Tiehl, N. Rucker, M. A. Schwarz, P. S. Gill and C. J. Gomer (2000) Antiangiogenic treatment enhances photodynamic therapy responsiveness in a mouse mammary carcinoma. *Cancer Res.* **60**, 4066–4069.
 18. Jaques, S. L., X.-Y. He and G. Gofstein (1993) Design of PDT protocols using delta-aminolevulinic acid (5ALA). *Proc. SPIE* **1881**, 99–108.
 19. Madsen, S. J., C. H. Sun, B. J. Tromberg and H. Hirschberg (2001) Development of a novel indwelling balloon applicator for optimizing light delivery in photodynamic therapy. *Lasers Surg. Med.* **29**, 406–412.
 20. Madsen, S. J., C. H. Sun, B. J. Tromberg, V. P. Wallace and H. Hirschberg (2000) Photodynamic therapy of human glioma spheroids using 5-aminolevulinic acid. *Photochem. Photobiol.* **72**, 128–134.
 21. Wilson, B. C., S. Bisland, A. Bogaards, A. Lin, E. Moriyama, K. Zhang and L. Lilge (2003) Metronomic photodynamic therapy (mPDT): concepts and technical feasibility in brain tumor. *Proc. SPIE* **4952**, 23–31.
 22. Edwards, S., D. Jackson, J. Reynoldson and B. Shanley (1984) Neuropharmacology of delta-aminolaevulinic acid. II. Effect of chronic administration in mice. *Neurosci. Lett.* **50**, 169–173.
 23. Mustajoki, P., K. Timonen, A. Gorchein, A. M. Seppalainen, E. Matikainen and R. Tenhunen (1992) Sustained high plasma 5-aminolaevulinic acid concentration in a volunteer: no porphyrin symptoms. *Eur. J. Clin. Investig.* **22**, 407–411.
 24. Van de Boogert, J., R. van Hillegersberg, F. W. de Rooij, R. W. de Bruin, A. Edixhoven-Bosdijk, A. B. Houtsmuller, P. D. Siersema, J. H. Wilson and H. W. Tilanus (1998) 5-Aminolaevulinic acid-induced protoporphyrin IX accumulation in tissues: pharmacokinetics after oral or intravenous administration. *J. Photochem. Photobiol. B: Biol.* **44**, 29–38.
 25. Stummer, W., A. Novotny, H. Stepp, C. Goetz, K. Bise and H. J. Reulen (2000) Fluorescence-guided resection of glioblastoma multiforme by using 5-aminolevulinic acid-induced porphyrins: a prospective study in 52 consecutive patients. *J. Neurosurg.* **93**, 1003–1013.
 26. Lilge, L., K. Menzies, A. Lin, S. K. Bisland and B. C. Wilson (2002) PDT-induced apoptosis: investigations using two malignant brain tumor models. *Proc. SPIE* **4612**, 136–142.
 27. Bisland, S. K., L. Lilge, A. Lin and B. C. Wilson (2003) Metronomic photodynamic therapy (mPDT) for intracranial neoplasm: physiological, biological, and dosimetry considerations. *Proc. SPIE* **5142**, 9–17.
 28. Bogaards, A., A. Varma, E. H. Moriyama, A. Lin, A. Giles, S. Bisland, L. Lilge, G. M. Bilbao, P. J. Muller and B. C. Wilson (2003) Fluorescence guided resection of intracranial VX2 tumor in a preclinical model using 5-aminolevulinic acid (ALA): preliminary results. *Proc. SPIE* **4952**, 91–96.
 29. The Canadian Council on Animal Care (1993). Control of animal pain in research, teaching and testing. In *Guide to the Care and Use of Experimental Animals*, Chapter 10, 2nd Ed, Vol 1 (Edited by E. D. Olfert, B. M. Cross and A. A. McWilliam), CCAC, Ottawa, Ontario, Canada.
 30. Lilge, L., C. O'Carroll and B. C. Wilson (1997) A solubilization technique for photosensitizer quantification in ex vivo tissue samples. *J. Photochem. Photobiol. B: Biol.* **39**, 229–235.
 31. van Hillegersberg, R., J. M. Hekking-Weijma, J. H. Wilson, A. Edixhoven-Bosdijk and W. J. Kort (1995) Adjuvant intraoperative photodynamic therapy diminishes the rate of local recurrence in rat mammary tumour model. *Br. J. Cancer* **71**, 733–737.
 32. Kennedy, J. C. and R. H. Pottier (1992) Endogenous protoporphyrin IX, a chemically useful photosensitizer for photodynamic therapy. *J. Photochem. Photobiol. B: Biol.* **14**, 275–292.
 33. Ennis, S. R., A. Novotny, J. Xiang, P. Shakui, T. Masada, W. Stummer, D. E. Smith and R. F. Keep, (2003) Transport of 5-aminolevulinic acid between blood and brain. *Brain Res.* **959**, 226–234.
 34. Garcia, S. C., M. B. Moretti, M. V. Garay and A. Batlle (1998) Delta-aminolevulinic acid transport through blood-brain barrier. *Gen. Pharmacol.* **31**, 579–582.
 35. Dereski, M. O., M. Chopp, J. H. Garcia and F. W. Hetzel (1991) Depth measurements and histopathological characterization of photodynamic therapy generated normal brain necrosis as a function of incident optical energy dose. *Photochem. Photobiol.* **54**, 109–112.
 36. Shah, K., Y. Tang, X. Breakefield and R. Weissleder (2003) Real-time imaging of TRAIL-induced apoptosis of glioma tumors *in vivo*. *Oncogene* **22**, 6865–6872.
 37. Moriyama, E. H., S. K. Bisland, A. Lin, A. Bogaards, L. Lilge and B. C. Wilson (2003). Bioluminescence monitoring of photodynamic therapy response of rat gliosarcoma *in vitro* and *in vivo*. *Proc. SPIE* **4952**, 76–81.
 38. Nagashima, G., R. Suzuki, H. Hokaku, M. Takahashi, T. Miyo, J.-I. N. Nakagawa and T. Fujimoto (1999) Graphic analysis of microscopic tumor cell infiltration, proliferative potential, and vascular endothelial growth factor expression in an autopsy brain with glioblastoma. *Surg. Neurol.* **51**, 292–299.
 39. Barth, R. F. (1998) Rat brain tumor models in experimental neuro-oncology: the 9L, C6, T9, F98, RG2 (D74), RT-2 and CNS-1 gliomas. *J. Neuro-oncol.* **36**, 91–102.
 40. Lobel, J., I. J. MacDonald, M. J. Ciesielski, T. Barone, W. R. Potter, J. Pollina, R. J. Plunkett, R. A. Fenstermaker and T. J. Dougherty (2001) 2-[1-hexyloxyethyl]-2-devinyl pyropheophorbide-a (HPPH) in a nude rat glioma model: implications for photodynamic therapy. *Lasers Surg. Med.* **29**, 397–405.